J. Fluid Mech. (1983), *vol.* 127, *pp.* 203–217
Printed in Great Britain

On the motion of a slender body near an interface between two immiscible liquids at very low Reynolds numbers

By G. R. FULFORD AND J. R. BLAKE
Department of Mathematics, The University of Wollongong, Wollongong, N.S.W. 2500, Australia

(Received 19 May 1981 and in revised form 2 August 1982)

The motion of a slender body near a flat interface between two immiscible fluids of different viscosities and densities is considered. The force distributions along a slender body are derived for the two cases when the instantaneous motion of the slender body is parallel to, and normal to, the interface. In some cases the slender body will rotate, the magnitude and direction of rotation being a function of the ratio of the two viscosities and the distance from the interface. For a narrow band of viscosity ratios the direction of rotation for a normally oriented slender body will change with distance from the interface. Two mechanisms for the interface-induced rotation are discussed.

1. Introduction

The motion of long slender bodies at very small Reynolds number occurs in many different areas of science and industry. Often these problems involve the presence of a plane boundary or a boundary which, under appropriate assumptions, may be taken to be approximately flat; for example a rigid plane wall, a free surface, or an interface between two immiscible fluids of different viscosities and densities.

Examples of slender bodies moving near these types of boundaries occur in the locomotion of micro-organisms, where the beating of long slender flagella or fields of hairlike cilia propel the organism through the surrounding fluid. In muco-ciliary transport in the lung, the beating of cilia transports mucus up the bronchial tubes. This system is often modelled as two separate layers of fluid – the watery lower serous layer, in which the cilia beat, and the more viscous upper mucous layer (see Blake 1975) to which foreign particles adhere and are thus removed from the lung. Other examples include polymer extrusion in the petrochemical industry, which involves slender fibres moving near a free surface, and also flotation processes where the behaviour of particles near the bubble free surface is important.

In elasticity theory, the fibre pull-out problem is similar to the previous examples (see Phan-Thien 1980). In this case, a rigid fibre is embedded in a semi-infinite elastic medium where one wishes to calculate the force required for a given displacement of the fibre. At this stage we wish to make a clear distinction between the boundary conditions for a flat free surface in elasticity (in which both the tangential and normal stress on the interface are zero) and in fluid mechanics (where the tangential stress and normal velocity are zero but there is a normal stress acting on the surface due to gravity or surface tension). We will be concerned with the latter case in this paper.

There have been a number of recent studies of the motion of particles in the presence of rigid plane wall boundaries. Brenner (1962) and Katz, Blake & Paveri-Fontana (1975) (see also Lighthill 1975) obtained expressions for the drag on a slender

body which were valid far from the wall and close to the wall respectively. It remained for de Mestre (1973) and de Mestre & Russel (1975) to provide continuity between the above two limiting cases. More recently, attention has been directed towards the behaviour of particles near interfaces. Lee, Chadwick & Leal (1979), Lee & Leal (1980) and O'Neill & Ranger (1979) have investigated the motion of translating and rotating spheres in the presence of a flat interface that separates two semi-infinite immiscible fluids. Thus there is a need to investigate the motion of other types of particles near an interface, and in particular, in view of the wide range of possible applications mentioned above, to examine the motion of a slender body near this type of boundary.

In this paper we extend de Mestre's (1973) and de Mestre & Russel's (1975) analysis from the rigid plane wall boundary to that of a flat interface between two semi-infinite immiscible fluids of different viscosities and densities. We consider an axisymmetric slender body oriented parallel to the interface and moving (i) axially (in the direction of the axis of symmetry of the body), (ii) transversely (in a direction normal to the axis of symmetry but parallel to the interface), (iii) normal to the interface; and a slender body oriented perpendicular to the interface and moving (iv) axially (and normal to the interface), and (v) transversely.

Using line distributions of stokeslets and higher-order singularities we obtain asymptotic expansions of the force distributions on the slender body for the above-mentioned cases. The perturbation parameter is $\epsilon = [\ln(2l/R_0)]^{-1}$, where the length of the body is $2l$ and a lengthscale for the radius of the cross-section is R_0, with $R_0 \ll l$. From the force distributions we can directly calculate the drag on the body and, in the case of motion parallel to the interface the angular velocity of the body (where the presence of the interface induces the body to rotate about its centre) as a function of the distance from the interface and the ratio of viscosities of the two fluids. It appears that line distributions of singularities will not adequately model the flow around the ends of the body (although they are very effective in modelling the rest of the flow) and it is suggested that a distribution of stokeslets over the whole surface of the body be used for the investigation of end effects.

In our theory we have assumed the interface to be perfectly flat, although in practice the motion of a slender body will distort the shape of the interface. However, we can find conditions under which the interface deformation is sufficiently small that it may be neglected. Assuming the deformation to be small, Aderogba & Blake (1978*b*) obtain expressions for a first-order approximation to the interface shape in the presence of a stokeslet, where the action of (i) a uniform interfacial tension (γ), and (ii) hydrostatic pressure due to a density difference $\rho_1 - \rho_2$, balances the normal stresses across the interface due to the action of the stokeslet. Using these expressions and exploiting the approximately uniform nature of the force distributions, we obtain the following conditions (corresponding to (i) and (ii) above) for the flat interface approximation to be valid:

$$\left.\begin{aligned} &\text{(i)} \quad \frac{\mu_1 U}{\gamma} = o\left(\frac{H}{l}\right), \\ &\text{(ii)} \quad \frac{\mu_1 U}{(\rho_1 - \rho_2) g H^2} = o\left(\frac{H}{l}\right). \end{aligned}\right\} \tag{1}$$

Here H is the distance from the interface to the nearest point on the slender body, μ_1 is the viscosity of the fluid in which the body is immersed, U is the velocity of the body and g is the acceleration due to gravity. It is clear from (1) that the flat-interface approximation is justified (even for close approaches) when the interfacial tension γ or the density difference $\rho_1 - \rho_2$ between the two fluids is very large.

2. Slender-body theory

A useful technique for solving problems involving Stokes flow around a body is to employ a distribution of singularities to represent the body. Past experience (Batchelor 1970) has shown us that for a slender body an approximate representation may be obtained from a line distribution of stokeslets along the axis of the body. This representation may be formulated from a surface integral solution of the Stokes equations by carrying out a Taylor-series expansion about the axis of the slender body, retaining only first-order terms (stokeslets). We shall not be concerned with such details here; however, further details of this procedure may be found in Russel & Acrivos (1972) and Chwang & Wu (1975). Thus using a centreline stokeslet distribution, the velocity field around a slender body (of length $2l$) may be approximated by

$$u_i(\mathbf{x}) = \int_{-l}^{l} F_j(s)\, G_{ij}(\mathbf{x}, s)\, ds, \tag{2}$$

where s measures distance along the centreline, $\mathbf{F}(x)$ is the distribution of force per unit length and G_{ij} is the Green function (which may be physically interpreted as the velocity field due to a unit point force acting along the jth coordinate axis). The accuracy of this representation may be improved by including higher-order singularities.

Our theory considers the motion of a slender body in a semi-infinite fluid of viscosity μ_1 and density ρ_1, above which lies a semi-infinite fluid of viscosity μ_2 and density ρ_2. The two fluids are separated by a flat interface, which we take to be the surface $x_3 = 0$. On the interface we require the normal velocity to be zero and the tangential velocities and stresses to be continuous across the interface. In order to apply slender-body theory we need a Green function G_{ij} that automatically satisfies these conditions. This Green function has been obtained by Aderogba & Blake (1978*a*) as

$$G_{ij} = \frac{1}{8\pi\mu_1}\left[\left(\frac{\delta_{ij}}{r} + \frac{r_i r_j}{r^3}\right) + \left(\frac{1-\theta}{1+\theta}\delta_{j\alpha}\delta_{\alpha k} - \delta_{j3}\delta_{3k}\right)\left(\frac{\delta_{ik}}{R} + \frac{R_i R_k}{R^3}\right)\right.$$
$$\left. + \frac{2\theta}{1+\theta}h(\delta_{j\alpha}\delta_{\alpha k} - \delta_{j3}\delta_{3k})\frac{\partial}{\partial R_k}\left(\frac{hR_i}{R^3} + \frac{\delta_{i3}}{R} + \frac{R_i R_3}{R^3}\right)\right] \tag{3}$$

$$(i, j, k = 1, \ldots, 3; \quad \alpha = 1, \ldots, 2; \quad x_3 < 0),$$

where h is the distance of the singularity from the interface, $\theta = \mu_2/\mu_1$ is the ratio of viscosities, and the coordinate vectors $\mathbf{r}$ and $\mathbf{R}$ are centred at the singularity ($x_3 = -h$) and its image point ($x_3 = h$) respectively.

The unknown force distribution $\mathbf{F}(s)$ in (2) can be determined by imposing the no-slip boundary condition on the surface of the slender body, which we assume is moving with a constant velocity $\mathbf{U}$. Substitution of this condition into (2) yields a set of simultaneous Fredholm integral equations of the first kind for the components of $\mathbf{F}(s)$.

The following analysis involves a slender body of length $2l$ and of circular cross-section (with radius r_0). We take the mid-point of the body to be a distance h from the interface. Two extreme orientations of the axis of the slender body are examined:

(i) parallel to the interface (see figure 1(*a*), in which case (using cylindrical polar coordinates r_0, ϕ, x)

$$\mathbf{r} = (x-s,\ r_0(x)\cos\phi,\ r_0(x)\sin\phi),$$
$$\mathbf{R} = (x-s,\ r_0(x)\cos\phi,\ r_0(x)\sin\phi - 2h)$$

on the surface of the body;

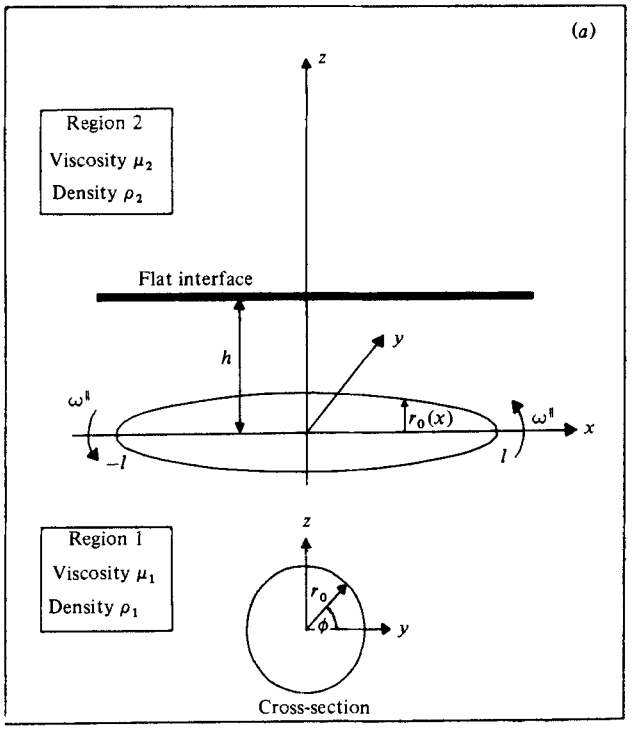

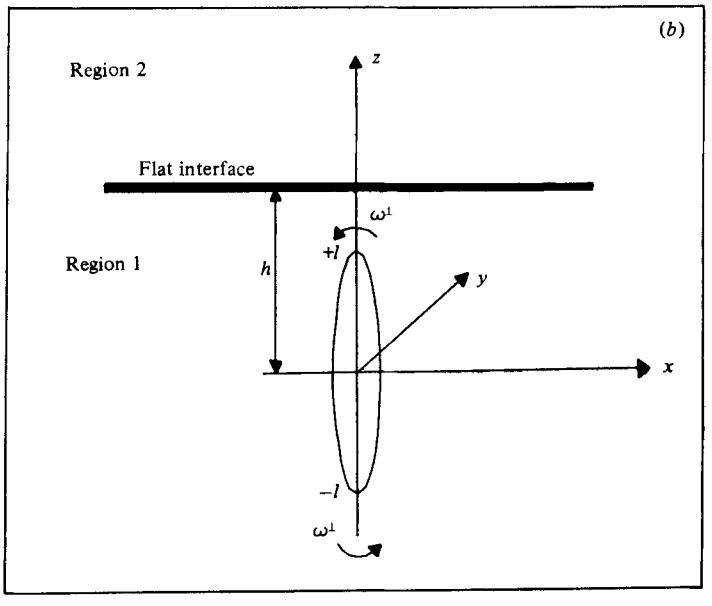

FIGURE 1. Illustration of the coordinate system for a slender body oriented (*a*) parallel, (*b*) perpendicular to the interface.

(ii) perpendicular to the interface (see figure 1*b*), where

$$\mathbf{r} = (r_0(x)\cos\phi,\ r_0(x)\sin\phi,\ z-s),$$
$$\mathbf{R} = (r_0(x)\cos\phi,\ r_0(x)\sin\phi,\ z+s-2h)$$

on the surface of the body.

To solve for the force distribution $\mathbf{F}(x)$ we take advantage of the slenderness of the body by expanding the integral equations to first order in R_0/l (and to first order in R_0/h for parallel orientations), where R_0 is the maximum radius of the circular cross-section of the body (note that there is no restriction on the relative magnitude of h and l). By averaging around the cross-section of the body, any remaining terms involving the polar angle ϕ are conveniently eliminated. Formally, these terms could have been cancelled out [to $O(R_0/l)$] by having originally included a distribution of potential source doublets along the axis of the body. The resulting integral equations are finally solved by making an asymptotic expansion for $\mathbf{F}$ of the form

$$\mathbf{F}(s) = \epsilon\mathbf{F}^{(1)} + \epsilon^2\mathbf{F}^{(2)} + \ldots, \tag{4}$$

where $\epsilon = [\ln(2l/R_0)]^{-1}$. Clearly ϵ is a small parameter when R_0/l is small. In the rest of this section solutions for $\mathbf{F}$ to $O(\epsilon^2)$ will be presented for both parallel and perpendicular orientations and for motion of the slender body along the three coordinate axes.

2.1. *Parallel orientation – axial motion*

We consider the slender body translating with speed U_1 along the x-axis (i.e. in the direction of the axis of symmetry of the body). De Mestre & Russel (1975) showed that the presence of a plane wall will induce the body to rotate such that its leading end moves away from the wall. We will assume that an external couple is acting on the body preventing it from rotating. This couple will be evaluated in §3. The distribution of force $\mathbf{F}$ on the body correct to $O(\epsilon^2)$ is given (in asymptotically correct form) by

$$F_1(x) = \frac{8\pi\mu_1 U_1 \epsilon}{4+\epsilon\{4S(x)-2-E_1(x;\theta)\}} + O(\epsilon^3), \tag{5a}$$

$$F_3(x) = \epsilon^2\pi\mu_1 U_1 G_1(x;\theta) + O(\epsilon^3) \tag{5b}$$

and the F_2 component vanishes like $O(R_0/l)$.

The effect of the interface is contained in the terms

$$E_1 = \frac{\theta-1}{\theta+1}\left(2\sinh^{-1}\frac{l-x}{2h} + 2\sinh^{-1}\frac{l+x}{2h} - \frac{l-x}{R_-} - \frac{l+x}{R_+}\right)$$
$$+ \frac{\frac{1}{2}\theta}{1+\theta}\left(\frac{l-x}{R_-} + \frac{l+x}{R_+} - \frac{(l-x)^3}{R_-^3} - \frac{(l+x)^3}{R_+^3}\right),$$

$$G_1 = \frac{2h}{1+\theta}\left(\frac{1}{R_-} - \frac{1}{R_+}\right) + \frac{4h^3}{1+\theta}\left(\frac{1}{R_-^3} - \frac{1}{R_+^3}\right),$$

with

$$R_-^2 = (l-x)^2 + 4h^2,$$
$$R_+^2 = (l+x)^2 + 4h^2,$$
$$S(x) = \ln\frac{(1-x^2/l^2)^{\frac{1}{2}}}{r_0(x)/R_0}.$$

In an infinite fluid one finds that only the component of $\mathbf{F}$ in the direction of motion

of the body is required. The presence of the interface necessitates the inclusion of an additional distribution of stokeslets directed normal to the interface. This is to take account of the reaction of the interface to the normal stress on the fluid induced by the flow around the body.

2.2. *Parallel orientation – transverse motion*

In this case the slender body is translating in the direction of the y-axis with velocity $\mathbf{U} = (0, U_2, 0)$. The solution for F_2 correct to $O(\epsilon^2)$ is

$$F_2(x) = \frac{8\pi\mu_1 U_2 \epsilon}{2+\epsilon\{2S(x)+1-E_2(x:\theta)\}} + O(\epsilon^3), \tag{6}$$

where

$$E_2 = \frac{\theta-1}{\theta+1}\left[\sinh^{-1}\frac{l-x}{2h} + \sinh^{-1}\frac{l+x}{2h}\right] + \frac{\frac{1}{2}\theta}{1+\theta}\left(\frac{l-x}{R_-} + \frac{l+x}{R_+}\right).$$

We found that an additional distribution of stokeslets normal to the interface is not required here. This is because the normal force is acting over a lengthscale of R_0 and is therefore negligible.

2.3. *Parallel orientation – normal motion*

The slender body is moving in the z-direction – i.e. towards the interface with velocity $\mathbf{U} = (0, 0, U_3)$. The force distribution is found to be

$$F_3(x) = \frac{8\pi\mu_1 U_3 \epsilon}{2+\epsilon\{2S(x)+1-E_3(x;\theta)\}} + O(\epsilon^3), \tag{7a}$$

$$F_1(x) = -\pi\mu_1 U_3 \epsilon^2 G_1(x;\theta) + O(\epsilon^3), \tag{7b}$$

where

$$E_3 = \sinh^{-1}\frac{l-x}{2h} + \sinh^{-1}\frac{l+x}{2h} + \frac{l-x}{R_-} + \frac{l+x}{R_+} + \frac{\theta}{1+\theta}\left(\frac{l-x}{R_-} + \frac{l+x}{R_+} - \frac{1}{2}\frac{(l-x)^3}{R_-^3} - \frac{1}{2}\frac{(l+x)^3}{R_+^3}\right),$$

with G_1 defined previously in (5). It was found that two stokeslet distributions were required – one in the direction of motion (F_3) and another in the x-direction (F_1), which represents the 'squeezing' effect on the fluid caused by the body moving towards the interface and thus forcing fluid along the surface of the slender body.

2.4. *Perpendicular orientation – axial motion*

The slender body is oriented perpendicular to the interface and moving towards it with velocity $\mathbf{U} = (0, 0, U_3)$. The force distribution is represented by

$$F_3(z) = \frac{8\pi\mu_1 U_3 \epsilon}{4+\epsilon\{4S(z)-2-E_4(z;\theta)\}} O(\epsilon^3), \tag{8}$$

where

$$E_4 = 2\ln\frac{2h+l-z}{2h-l-z} + \frac{\theta}{1+\theta}\left\{\frac{8l(z-h)(hz-2h^2+l^2)}{[(z-2h)^2-l^2]^2}\right\}.$$

2.5. *Perpendicular orientation – transverse motion*

We consider the slender body translating in the direction of the x-axis with velocity $\mathbf{U} = (U_1, 0, 0)$. By symmetry this is equivalent to the body moving in the y-direction. The force distribution is given by

$$F_1(z) = \frac{8\pi\mu_1 U_1 \epsilon}{2+\epsilon\{2S(z)+1-E_5(z;\theta)\}}, \tag{9}$$

where

$$E_5 = \frac{\theta-1}{\theta+1}\ln\frac{2h+l-z}{2h-l-z} + \frac{\theta}{1+\theta}\frac{4l(z-h)(hz-2h^2+l^2)}{[(z-2h)^2-l^2]^2}.$$

Note that in this case (as well as in §2.1) we have found it convenient to nullify the interface-induced rotation by imposing an external couple on the body.

3. The interface-induced drag and angular velocity of a slender body

The drag on a slender body in the presence of a flat interface can be calculated for the examples discussed in §2. This is achieved by integrating the force distributions over the length of the body, i.e.

$$\mathbf{D} = \int_{-l}^{l} \mathbf{F}(\sigma)\, d\sigma. \tag{10}$$

The integration is most easily accomplished by transferring the interface effect terms of (5)–(9) to the numerator (incurring an error of ϵ^3). Care must be taken to ensure that terms of the form ϵE_1 are $o(1)$.

The drag on the slender body correct to $O(\epsilon^2)$ is given by

$$D = \frac{4\pi\mu_1 Ul}{\ln(2l/R_0)+c^*-\frac{1}{2}I} \tag{11}$$

for axial motion, and

$$D = \frac{8\pi\mu_1 Ul}{\ln(2l/R_0)+c^*+1-\frac{1}{2}I} \tag{12}$$

for transverse motion, where c^* is defined by

$$c^* = -\tfrac{1}{2} + \frac{1}{2l}\int_{-l}^{l} S(x)\, dx. \tag{13}$$

This constant takes different values for different shaped bodies (e.g. for a cylinder $c^* = -0{\cdot}81$, for a prolate spheroid $c^* = -\frac{1}{2}$). The interface effect terms (labelled I in (11) and (12)) for the various orientations considered in this paper are

$$I_1^{\parallel} = \frac{\theta-1}{\theta+1}\left(2\sinh^{-1}\frac{l}{h} - 3\left(1+\frac{h^2}{l^2}\right)^{\frac{1}{2}} + \frac{3h}{l}\right) + \frac{\theta}{\theta+1}\left(\frac{1}{2}\frac{h}{l} - \frac{h^2}{2l^2}\left(1+\frac{h^2}{l^2}\right)^{-\frac{1}{2}}\right), \tag{14a}$$

$$I_2^{\parallel} = \frac{\theta-1}{\theta+1}\left(2\sinh^{-1}\frac{l}{h} - 2\left(1+\frac{h^2}{l^2}\right)^{\frac{1}{2}} + \frac{2h}{l}\right) + \frac{\theta}{\theta+1}\left[\left(1+\frac{h^2}{l^2}\right)^{\frac{1}{2}} - \frac{h}{l}\right], \tag{14b}$$

$$I_3^{\parallel} = 2\sinh^{-1}\frac{l}{h} + \frac{\theta}{\theta+1}\left(1+\frac{h^2}{l^2}\right)^{-\frac{1}{2}} \tag{14c}$$

for parallel orientation, and

$$I_4^{\perp} = \left[\left(\frac{h}{l}+1\right)\ln\left(1+\frac{l}{h}\right)+\left(\frac{h}{l}-1\right)\ln\left(1-\frac{l}{h}\right)\right]+\frac{1}{2}\frac{\theta}{\theta+1}\frac{l}{h}, \tag{14d}$$

$$I_5^{\perp} = \frac{\theta-1}{\theta+1}\left[\left(\frac{h}{l}+1\right)\ln\left(1+\frac{l}{h}\right)+\left(\frac{h}{l}-1\right)\ln\left(1-\frac{l}{h}\right)\right]+\frac{1}{2}\frac{\theta}{\theta+1}\frac{l}{h} \tag{14e}$$

for perpendicular orientation. It is noted that for $\theta = \infty$ the above results agree with de Mestre & Russel's (1975) calculations for a rigid plane boundary.

The far-field limit of these expressions is obtained by letting l/h tend to zero (i.e. the distance of the body from the interface is much greater than the length of the body). Then

$$I_1^{\parallel} = \frac{l}{h}\left(\frac{3}{4}\frac{\theta}{\theta+1}-\frac{\frac{1}{2}}{\theta+1}\right)+O\left(\frac{l^3}{h^3}\right), \tag{15a}$$

$$I_2^{\parallel} = \frac{l}{h}\left(\frac{3}{2}\frac{\theta}{\theta+1}-\frac{1}{\theta+1}\right)+O\left(\frac{l^3}{h^3}\right), \tag{15b}$$

$$I_3^{\parallel} = \frac{l}{h}\left(3\frac{\theta}{\theta+1}+2\frac{1}{\theta+1}\right)+O\left(\frac{l^3}{h^3}\right), \tag{15c}$$

$$I_4^{\perp} = \frac{l}{h}\left(\frac{3}{2}\frac{\theta}{\theta+1}+\frac{1}{\theta+1}\right)+O\left(\frac{l^3}{h^3}\right), \tag{15d}$$

$$I_5^{\perp} = \frac{l}{h}\left(\frac{3}{2}\frac{\theta}{\theta+1}-\frac{1}{\theta+1}\right)+O\left(\frac{l^3}{h^3}\right). \tag{15e}$$

Both the $\theta = \infty$ and $\theta = 0$ cases agree with Brenner's (1962) results.

An interesting feature of these equations is the relative magnitude of the drag on a slender body in the presence of a flat interface compared with that in an infinite fluid (where the drag coefficients can be obtained from (11) and (12) by setting I equal to zero). This can be seen clearly in the far field ($l/h \ll 1$) (where the effect of the interface is minimal): the drag is greater than with an infinite fluid for all values of θ in the case of motion normal to the interface, but for transverse and longitudinal motion the drag is smaller for values of θ near zero and greater for large values of θ. The critical value of θ where the drag is equal to the drag in an infinite fluid occurs at $\theta = \frac{2}{3}$. This result is the same as that obtained by Lee *et al.* (1979) for the drag on a sphere in the presence of an interface. Thus for a sufficiently large distance from the interface, when calculating the effect of the interface on the drag, both the orientation and shape of a particle are unimportant.

For close approaches to the interface ($r_0 \ll h \ll l$) the drag reduces to

$$D_1^{\parallel} = \frac{4\pi\mu_1 U_1}{\ln\frac{2l}{R_0}+c^*-\frac{\theta-1}{\theta+1}\left(\ln\frac{l}{h}+\ln 2-\frac{3}{2}\right)}+O\left(\frac{h}{l}\right), \tag{16a}$$

$$D_2^{\parallel} = \frac{8\pi\mu_1 U_1}{\ln\frac{2l}{R_0}+c^*+1-\frac{\theta-1}{\theta+1}\left(\ln\frac{l}{h}+\ln 2-1\right)-\frac{\frac{1}{2}\theta}{\theta+1}}+O\left(\frac{h}{l}\right), \tag{16b}$$

$$D_3^{\parallel} = \frac{8\pi\mu_1 U_1}{\ln\frac{2h}{R_0}+c^*+1-\ln 2-\frac{\frac{1}{2}\theta}{\theta+1}}+O\left(\frac{h}{l}\right), \tag{16c}$$

$$D_4^{\perp} = \frac{4\pi\mu_1 U_1}{\ln\dfrac{2l}{R_0} + c^* - \ln 2 - \dfrac{1}{4}\dfrac{\theta}{\theta+1}} + O\left(\frac{h-1}{l}\right), \tag{16d}$$

$$D_5^{\perp} = \frac{8\pi\mu_1 U_1}{\ln\dfrac{2l}{R_0} + c^* + 1 - \dfrac{\theta-1}{\theta+1}\ln 2 - \dfrac{1}{4}\dfrac{\theta}{\theta+1}} + O\left(\frac{h-l}{l}\right). \tag{16e}$$

Equations (16*a–c*) are in agreement with the results of Blake (1974*b*) for $\theta = \infty$. For perpendicular orientations with $h/l \to 1$ one end of the slender body is very close to the interface. A more accurate modelling of this case could be carried out using a surface distribution approach.

Both the far-field and near-field approximations together with the drag on a slender body oriented parallel to a rigid plane wall ($\theta = \infty$) and moving in the x-direction are plotted in figure 2 (*a*). The near-field expression asymptotes to the drag from below, whereas the far-field expression asymptotes from above. This is true for all values of θ and also for the other cases considered here. The far-field expressions are seen to be quite accurate down to about one body length away ($h/l = 2$) and so may prove to be very useful in resistive-force theory.

In figure 2 (*b*) we have plotted the drag on a slender body for each of the five cases considered here for $\theta = 0$ and $\theta = \infty$. The interface effect on the drag for the slender body oriented perpendicular to the interface is less than that for the slender body oriented parallel to the interface (especially closer to the interface) because more of the body is further away from the interface. The most notable result is the rapid increase in drag as the end of the body gets within half a body length from the interface.

It was pointed out in §2 that an external couple needs to be applied to a slender body moving in the x-direction to prevent it from rotating. Alternatively we could have allowed the slender body to rotate and calculate the instantaneous angular velocity ω by requiring the couple on the body about its centre to be zero. This requires us to modify the force distributions given in (5) and (9) by adding $2\pi\mu_1 \epsilon\omega x$ to F_1 and $4\pi\mu_1 \epsilon\omega x$ to F_3 in (5) and adding $-2\pi\mu_1 \epsilon\omega z$ to F_3 in (9). The error in each case remains $O(\epsilon^3)$. Thus the interface-induced angular velocity of a slender body oriented parallel to the interface is

$$\omega^{\parallel} = -\frac{3U_1\epsilon h^2}{2l^3}\left\{\frac{2}{1+\theta}\left(1-\left(1+\frac{l^2}{h^2}\right)^{\frac{1}{2}}+\frac{l}{2h}\sinh^{-1}\frac{l}{h}\right)+\frac{\theta}{1+\theta}\left(\frac{1+l^2/2h^2}{(1+l^2/h^2)^{\frac{1}{2}}}-1\right)\right\}+O(\epsilon^2), \tag{17}$$

and perpendicular to the interface it is

$$\omega^{\perp} = -\frac{3U_1\epsilon}{4l}\left\{\frac{2}{1+\theta}\left[\frac{h}{l}\left(\frac{h}{l}+1\right)\ln\left(1+\frac{l}{h}\right)+\frac{h}{l}\left(\frac{h}{l}-1\right)\ln\left(1-\frac{l}{h}\right)-1\right]\right.$$
$$\left.-\frac{\theta}{1+\theta}\left[1+\left(\frac{h^2}{l^2}-1\right)\ln\left(1-\frac{l^2}{h^2}\right)\right]\right\}+O(\epsilon^2). \tag{18}$$

In the $\theta \to \infty$ limit (i.e. as the viscosity of the upper fluid $\mu_2 \to \infty$) the above expressions agree with de Mestre & Russel's (1975) angular velocities or a slender body near a rigid plane wall (except for a factor of $\frac{1}{2}$ in the $\omega^{\parallel}$ case which resulted from an error in de Mestre & Russel's corresponding expression for F_3).

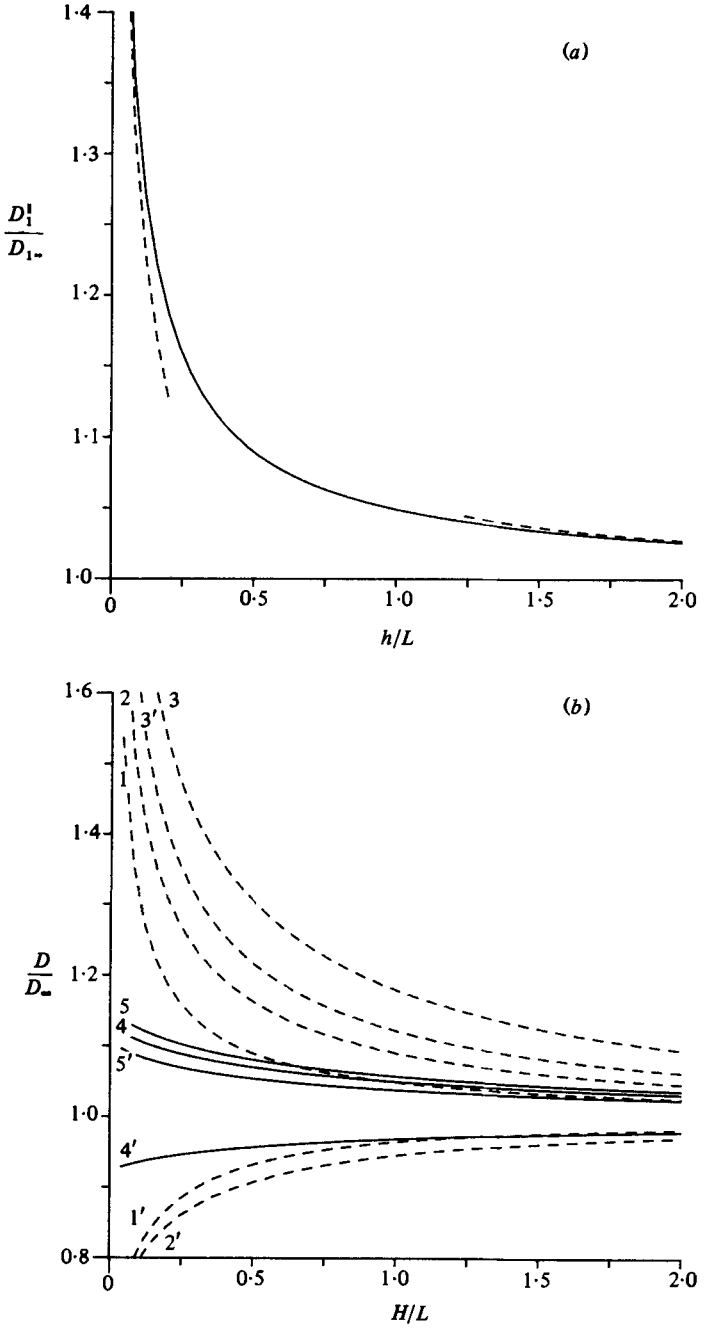

FIGURE 2. The drag on a slender body ($R_0/l = 0{\cdot}001$) (normalized with respect to the drag in an infinite fluid). (*a*) The body is oriented parallel to a rigid wall ($\theta = \infty$) and is moving in the x-direction. The dashed lines are the near- and far-field asymptotes. (*b*) A comparison of the effects of orientation and ratio of viscosity. The dashed lines represent parallel orientation and the solid lines perpendicular orientation. Unprimed numbers are for $\theta = \infty$ and primed for $\theta = 0$. The quantity H is given by h for parallel orientation and $h-l$ for perpendicular orientation.

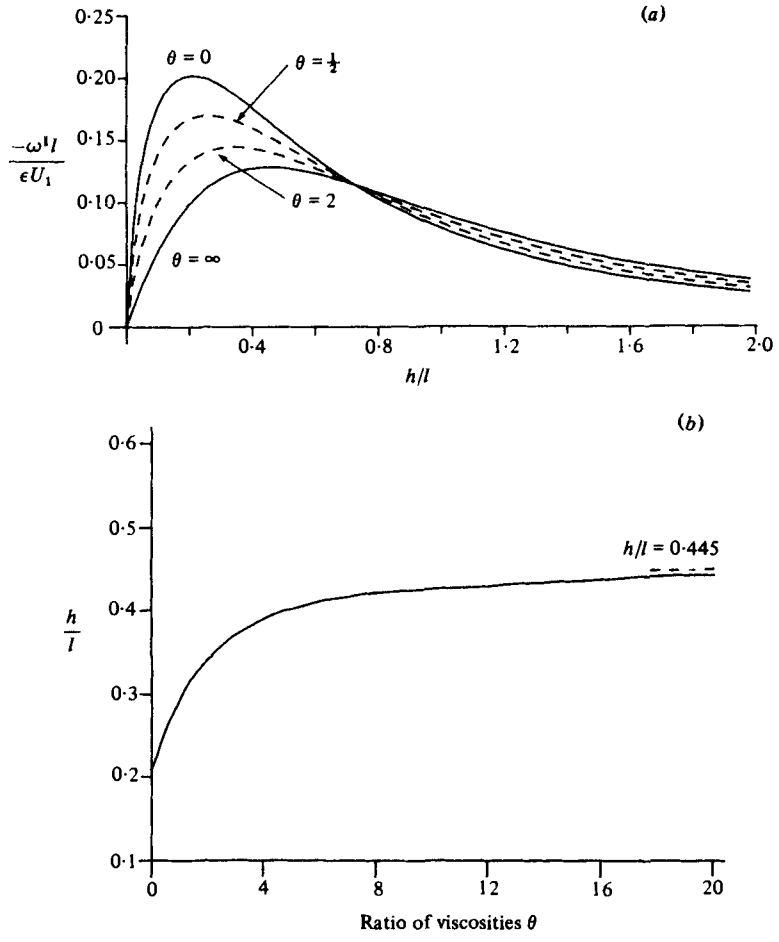

FIGURE 3. The angular velocity of a slender body that is oriented *parallel* to the interface. (*a*) Angular velocity *vs.* distance from interface. (*b*) The critical distance from the interface for which ω is a maximum *vs.* the ratio or viscosities of the two fluids.

Far-field limits for these expressions are obtained by letting $l/h \to 0$, i.e.

$$\omega^{\parallel} = -\frac{3U_1\epsilon}{l}\left\{\frac{2}{1+\theta}\frac{1}{48}\left(\frac{l}{h}\right)^2 + \frac{\theta}{1+\theta}\frac{1}{16}\left(\frac{l}{h}\right)^2\right\}, \tag{19}$$

$$\omega^{\perp} = -\frac{3U_1\epsilon}{l}\left\{\frac{2}{1+\theta}\frac{1}{24}\left(\frac{l}{h}\right)^2 - \frac{\theta}{1+\theta}\frac{1}{8}\left(\frac{l}{h}\right)^2\right\}. \tag{20}$$

For parallel orientation, $\omega^{\parallel}$ is always less than zero for all values of θ and h (i.e. the leading end of the body rotates away from the interface). From an analysis of (19) or from figure 3(*a*) it can be seen that the angular velocity of the slender body diminishes as the distance from the interface increases (since at a large distance from the interface the body will behave as if it were in an infinite fluid). Close to the interface the angular velocity also tends to zero. Thus $|\omega|$ attains a maximum for a given value of the distance from the interface h and the ratio of viscosities θ, as illustrated in figure 3(*b*).

For parallel orientation $\omega^{\perp}$ tends to a finite limit as the slender body moves closer to the interface (i.e. as $h/l \to 1$), although the neglected end effects may be important

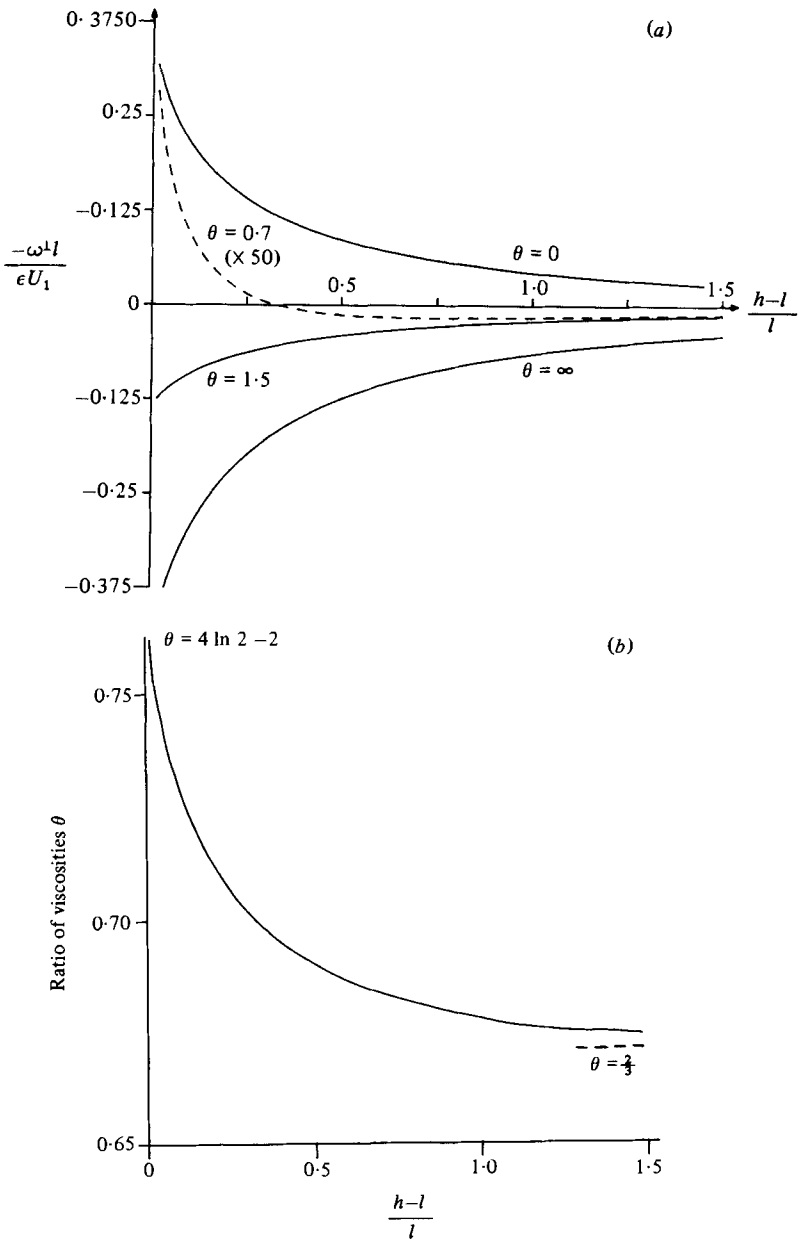

FIGURE 4. The angular velocity of a slender body that is oriented *perpendicular* to the interface. (*a*) Angular velocity *vs.* distance from interface. The dashed line has been magnified to illustrate the changing of direction of rotation. (*b*) Critical values of distance from the interface and the ratio of viscosities of the two fluids for which the angular velocity is zero.

here. In the free-surface case ($\theta = 0$) $\omega < 0$, while in the plane wall case ($\theta = \infty$) $\omega > 0$. Clearly for some intermediate value of θ there exists a value of h for which there is no rotation of the slender body in this particular orientation. In figure 4(*a*), the dimensionless angular velocity is plotted against distance from the interface for several values of θ, and in particular for $\theta = 0{\cdot}7$, where the direction of rotation changes with h/l. In figure 4(*b*), the ratio of viscosities as a function of h/l for which

$\omega = 0$ is illustrated. The range of θ for which this change of direction of rotation occurs is very small, being between $\frac{2}{3}$ and $4\ln 2 - 2$ (≈ 0.773). This result suggests the possibility of a capture region near an interface with an appropriate value of θ.

It should be emphasized that the case $\theta = 1$ (i.e. when the viscosities of the two fluids are equal) is not identical with that of a slender body translating in an infinite fluid since there is an implied distribution of normal stress on the surface $x_3 = 0$. This situation is probably unrealistic in practice, although theoretically it could occur between two fluids of the same viscosity but a large density difference.

4. Discussion

The rotation of a particle induced by its movement parallel to a flat interface appears to derive from a combination of two different mechanisms. When the particle is a slender body one of these two types of rotation will be negligible, depending on whether the axis of the slender body is oriented perpendicular or parallel to the interface.

When the slender body is oriented perpendicular to the interface the body rotates in response to a viscous-drag gradient along the slender body (the force/unit length on one part of the body will be different from that on another). We have seen in §3 that for a free surface ($\theta = 0$) the existence of a substantial slip velocity on the interface means that the viscous resistance will be smaller for those parts of the body closer to the interface, and thus the body will rotate in a clockwise direction. The opposite will be true for a rigid plane wall ($\theta = \infty$) owing to the absence of a slip velocity on the interface. We may also conclude from this explanation that the magnitude of the angular velocity will decrease as the distance of the slender body increases and that the direction of rotation might change for given values of h and θ. (These conclusions are confirmed in figure 4 (*a*), (*b*), although it is difficult to predict the restricted range of values of θ ($\approx 0{\cdot}66$–$0{\cdot}77$) for which $\omega^{\perp}$ is zero.)

A completely different mechanism for interface-induced rotation operates for the slender body oriented parallel to the flat interface, due primarily to the zero-normal-velocity condition on the interface. Thus the rotation will be in the same direction for all values of the viscosity of the upper fluid (i.e. ranging from the free-surface case $\theta = 0$ through to the rigid boundary $\theta = \infty$). As the slender body moves forward, fluid will be pushed outwards and away from the boundary at the front, whereas at the rear fluid will be pulled in towards the slender body. This implies an asymmetry in the fluid velocity field normal to the interface, which indicates either a couple acting on the slender body or a rotation such that the leading edge moves away from the interface. This explanation is consistent with figure 3 (*a*) since if the slender body is close to the interface the fluid flow in the region between the slender body and the flat interface will be almost unidirectional (i.e. the normal velocity will be very small) and thus the angular velocity will tend to zero as h tends to zero.

The problem of a sphere moving parallel to a flat interface was studied by Lee *et al.* (1979) (who assumed that the distance of the sphere from the interface was large) and Lee & Leal (1980) (whose solution was valid at all distances from the interface). These authors suggested that the interface-induced rotation of the sphere was due to the difference in velocity gradients above and below the sphere (this is the mechanism that causes the slender body oriented perpendicular to the interface to rotate). Our results indicate however that the second mechanism described above associated with $\omega^{\parallel}$) would also affect the rotation of a sphere. In the far field, (15), we note that for $\theta = \infty$ (a rigid plane-wall boundary) the angular velocities $\omega^{\parallel}$ and

$\omega^{\perp}$ of the slender bodies are of opposite sign, whereas for $\theta = 0$ (a flat free-surface boundary) they are of the same sign. From these results we expect that for a sphere the contributions of these two angular velocities will cancel for $\theta = \infty$, leaving a term $O(l/h)^4$ and for $\theta = 0$ they will add together to give a term of $O(l/h)^2$ as was obtained by Lee *et al.* (1979). Thus it appears that the interface-induced rotation of a body is made up of two separate rotation mechanisms, the combination of which depends on both the shape and the orientation of the body.

We can use our results for a slender body, in particular figures 3(*a*) and 4(*a*), to gain some further insight into the interface-induced rotation of a particle. If a particle is close to the interface the rotation will be derived from what we have called mechanism 1 (since $\omega^{\parallel}$ is small) and the direction of rotation will be dependent on the ratio of viscosities of the two fluids (and there will exist some critical value of θ where the angular velocity changes sign). As the particle moves further from the interface, however, mechanism 2 will become more important (the contribution being in the opposite direction to that induced by mechanism 1 if $\theta = 0$) and the critical value of θ will increase. This result was also obtained by Lee & Leal (1980) for a sphere.

Using the results for a slender body oriented parallel or perpendicular to a flat interface we have been able to predict qualitatively some of the results of Lee & Leal (1980) for the motion of a sphere near an interface. These studies will contribute to a greater understanding of the motion of differently shaped particles near an interface, which in turn will assist studies in many different fields such as colloid mechanics and muco-ciliary transport where the movement of small bodies near boundaries is of fundamental importance.

Part of this work was carried out (by G.R.F.) while a student in the Department of Applied Mathematics at the Australian National University, Canberra.

REFERENCES

ADEROGBA, K. & BLAKE, J. R. 1978*a* Action of a force near the planar surface between two semi-infinite immiscible liquids at very low Reynolds' numbers. *Bull. Aust. Math. Soc.* **18**, 345–356.

ADEROGBA, K. & BLAKE, J. R. 1978*b* Addendum to: Action of a force near the planar surface between two semi-infinite immiscible liquids at very low Reynolds numbers. *Bull. Aust. Math. Soc.* **19**, 309–318.

BATCHELOR, G. K. 1970 Slender-body theory for particles of arbitrary cross-section in Stokes flow. *J. Fluid Mech.* **44**, 419–440.

BLAKE, J. R. 1974*a* Fundamental singularities of viscous flow. Part I: The image systems in the vicinity of a stationary no-slip boundary. *J. Engng Math.* **8**, 23–29.

BLAKE, J. R. 1974*b* Singularities of viscous flow, Part II; Applications to slender body theory. *J. Engng Math.* **8**, 113–124.

BLAKE, J. R. 1975 On the movement of mucus in the lung. *J. Biomech.* **8**, 179–190.

BRENNER, H. 1962 Effect of finite boundaries on the Stokes' resistance of an arbitrary particle. *J. Fluid Mech.* **12**, 35.

CHWANG, A. T. & WU, T. 1975 Hydromechanics of low Reynolds number flow. Part 2. Singularity method for Stokes flow. *J. Fluid Mech.* **67**, 787–815.

KATZ, D. F., BLAKE, J. R. & PAVERI-FONTANA, S. L. 1975 On the movement of slender bodies near plane boundaries at low Reynolds number. *J. Fluid Mech.* **72**, 529–540.

LEE, S. H., CHADWICK, R. S. & LEAL, L. G. 1979 Motion of a sphere in the presence of a plane interface, Part I. An approximate solution by generalization of the method of Lorentz. *J. Fluid Mech.* **93**, 705–726.

LEE, S. H. & LEAL, L. G. 1980 Motion of a sphere in the presence of a plane interface, Part 2. An exact solution in bipolar coordinates. *J. Fluid Mech.* **98**, 193–224.

LIGHTHILL, J. 1975 *Mathematical Biofluidynamics.* S.I.A.M.

MESTRE, N. J. DE 1973 Low Reynolds number fall of slender cylinders near boundaries. *J. Fluid Mech.* **58**, 641–656.

MESTRE, N. J. DE & RUSSEL, W. B. 1975 Low Reynolds number translation of a slender cylinder near a plane wall. *J. Engng Math.* **9**, 81–91.

O'NEILL, M. E. & RANGER, K. B. 1979 On the rotation of a rotlet or sphere in the presence of an interface. *Int. J. Multiphase Flow* **5**, 143–148.

PHAN-THIEN, N. 1980 A contribution to the rigid fibre pull-out problem. *Fibre Sci. Tech.* **13**, 179–186.

RUSSEL, W. B. & ACRIVOS, A. 1972 On the effective moduli of composite materials; slender rigid inclusions at dilute concentrations. *Z. angew. Math. Phys.* **23**, 434–464.

RUSSEL, W. B., HINCH, E. J., LEAL, L. G. & TIEFFENBRUCH, G. 1977 Rods falling near a vertical wall. *J. Fluid Mech.* **83**, 273–287.